Comparing Black-Box Differential Evolution and Classic Differential Evolution: Revisited Investigation of Invariance to Rotation

Technical Report IJS-DP 12585

Delovno poročilo IJS-DP 12585

Aljoša Vodopija[1,2], Tea Tušar[1], Bogdan Filipič[1,2]
[1]Department of Intelligent Systems, Jožef Stefan Institute
Jamova cesta 39, SI-1000 Ljubljana, Slovenia
[2]Jožef Stefan International Postgraduate School
Jamova cesta 39, SI-1000 Ljubljana, Slovenia
{*aljosa.vodopija, tea.tusar, bogdan.filipic*}*@ijs.si*

September 2018

Abstract

We revisit our previous work on comparing black-box differential evolution (BBDE) and classic differential evolution, where we observed an unexpected residual sensitivity to rotation of BBDE. A detailed analysis of the results shows that it stems from a constraint handling technique that favours separability. Equipped with these findings, we re-designed our experiments by using only unbounded decision spaces. The new results show that for unbounded decision spaces BBDE is indeed invariant to rotation. In addition, we corrected the pseudocode of the 'target-to-best' variants, since we found out that they were written incorrectly in the original paper.

Contents

1 Introduction **3**

2 Observations on the original paper **3**
2.1 Invariance to rotation 3
2.2 The ‘target-to-best’ strategies 4

3 Revisited experimental setup and results **4**
3.1 Invariance to rotation 4
3.2 Results 4

4 Conclusions **5**

References **9**

1 Introduction

This report presents a revisited study of our previous work [1], where we compared black-box differential evolution (BBDE) [2] with classic differential evolution (DE) [3] using the COCO platform [4]. Reading the original paper is a precondition for understanding the following text.

In the original work, the experiments on separable and rotated variants of the ellipsoid problem (problems f_2 and f_{10} of the `bbob` test suite [5]) have demonstrated that while the BBDE variants are less sensitive to rotation than the DE variants, some sensitivity to this transformation still persists. The reason for this sensitivity remained unexplained. In addition, we realized that in the original paper the pseudocode describing DE/target-to-best and BBDE/target-to-best variants were incorrect.

In this study, we re-investigate the invariance to rotation of the BBDE variants and correct the pseudocode representing DE/targe-to-best and BBDE/target-to-best. By examining the results obtained in the previous work and experimenting with different settings we discover that the sensitivity to rotation was a consequence of using bounded decision spaces and a constraint handling technique favoring separability.

The rest of this report is organized as follows. Section 2 provides two observations on the original paper, while Section 3 presents the revisited experiments and their results. Section 4 concludes the report.

2 Observations on the original paper

2.1 Invariance to rotation

In the original experiments, decision spaces were bounded with box constraints. A feasible solution $p = (x_1, \ldots x_D)^{\mathrm{T}}$ satisfied the following constraints: $-5 \leq x_i \leq 5$ for all $i \in \{1, \ldots, D\}$. In order to satisfy these constraints, a constraint handling technique, replacing any infeasible component of the solution with a randomly selected feasible value, was used.

Figure 1 shows an example describing how an infeasible solution (red point) is replaced with a feasible one (black point). In this two-dimensional example the infeasible solution violates the x_1-constraint only. The constraint handling technique replaces x_1^1 with a randomly selected feasible value from $[-5, 5]$ keeping the value of x_2^1 intact. This specific constraint handling technique implicitly imposes an exploration bias toward searching in directions aligned with coordinate system axes. In other words, an optimizer using a similar constraint handling technique would show superior performance on separable problems.

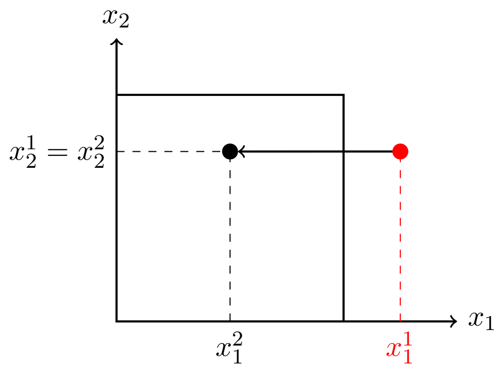

Figure 1: The constraint handling technique replacing the infeasible solution (red point) with a feasible one (black point). The direction of replacing the infeasible solutions is aligned with the x_1-axis.

Figure 2 shows the results of the original experiments obtained for the two ellipsoid problems in 20 dimensions. The BBDE performance is slightly better on the separable problem. Examining the results in more detail we find that about 26% of generated solutions for the ellipsoid problem have at least one infeasible value. In other words, in 26% of the cases the constraint handling technique imposes a bias towards searching in separable directions.

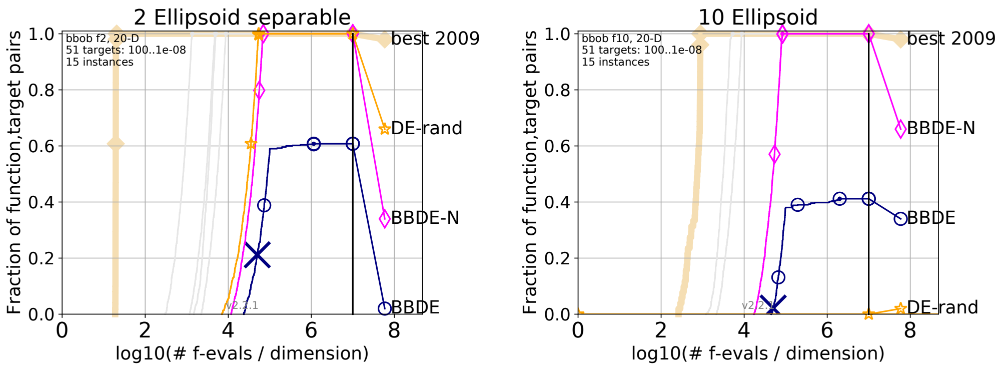

(a) Separable ellipsoid, f_2, dimension 20

(b) Rotated ellipsoid, f_{10}, dimension 20

Figure 2: ECDFs of simulated (bootstrapped) runtimes of the 'rand' strategy for separable (left) and rotated (right) ellipsoid and dimension 20. The yellow line indicates DE/rand, the purple line BBDE-N, and the blue line BBDE.

2.2 The 'target-to-best' strategies

The general form of the DE used in our work is shown in Algorithm 1. In the original paper, the pseudocode of the DE/target-to-best and BBDE/target-to-best variants was incomplete. The paper incorrectly stated that the trial vector is created as

$$p_{\text{trial}} = p + F \cdot (p_{\text{best}} - p)$$

in DE/target-to-best and as

$$p_{\text{trial}} = p + F \cdot (p_{\text{best}} - p_2)$$

in BBDE/target-to-best. Is this report, we present the correct pseudocode in Algorithms 2 and 3, respectively.

3 Revisited experimental setup and results

3.1 Invariance to rotation

In this revisited study, decision spaces are unbounded in all the experiments. Thus, any solution generated by any algorithm is feasible, and therefore no constraint handling technique needs to be used. However, the initial population is generated in such a way that its solutions lie in $[-5, 5]^D$. All other settings are equal to those from the original experiments.

3.2 Results

The overall performance of the DE and BBDE variants on bounded and unbounded decision spaces is shown in Figures 3, 5, and 7. We can observe that the results of the revisited experiments are almost identical to those in the original experiments. For this reason, no additional comments are provided here (the interested reader is referred to the original paper [1]).

Algorithm 1 DE

Input: population size and stopping criterion;
Output: population $\mathbb{P}$ of solutions;

create the initial population $\mathbb{P}$ of random solutions;
evaluate the solutions in $\mathbb{P}$;
while stopping criterion not met **do**
  $\mathbb{P}_{\text{new}} \leftarrow \emptyset$;
  for all $p \in \mathbb{P}$ **do**
    create a trial vector p_{trial};
    ensure feasibility of p_{trial};
    evaluate p_{trial};
    if p_{trial} is better than p **then**
      $p \leftarrow p_{\text{trial}}$;
    end if
    $\mathbb{P}_{\text{new}} \leftarrow \mathbb{P}_{\text{new}} \cup \{p\}$;
  end for
  $\mathbb{P} \leftarrow \mathbb{P}_{\text{new}}$;
end while
return $\mathbb{P}$;

Algorithm 2 Trial vector creation by DE/target-to-best

Input: population $\mathbb{P}$ and target vector $p \in \mathbb{P}$;
Output: trial vector p_{trial};

randomly select two different solutions $p_1, p_2 \in \mathbb{P}$;
create a trial vector $p_{\text{trial}} = p + F \cdot (p_{\text{best}} - p) + F \cdot (p_1 - p_2)$;
alter p_{trial} by crossover with p;
return p_{trial};

Algorithm 3 Trial vector creation by BBDE/target-to-best

Input: population $\mathbb{P}$ and target vector $p \in \mathbb{P}$;
Output: trial vector p_{trial};

randomly select two different solutions $p_1, p_2 \in \mathbb{P}$;
sample a scaling factor F from $X_F \sim \exp(\mathcal{N}(0,1))$;
create a trial vector $p_{\text{trial}} = p + F \cdot (p_{\text{best}} - p) + F \cdot (p_1 - p_2)$;
return p_{trial};

In contrast, from Figures 4, 6, and 8 it is evident that while the DE variants are highly sensitive to rotation, the performance of the BBDE variants is equal on separable and rotated ellipsoid problems when the decision space is unbounded. We can conclude that the observed sensitivity to rotation in our original experiments was a consequence of using a constraint handling technique favoring separability.

4 Conclusions

In this study, we re-investigated the rotational invariance of BBDE. We found that the rotational sensitivity observed on the ellipsoid problem is due to a constraint handling technique favoring separability. By re-designing our experiments so that unbounded decision spaces are used instead of bounded ones, we showed that for unbounded decision spaces the performance of BBDE is

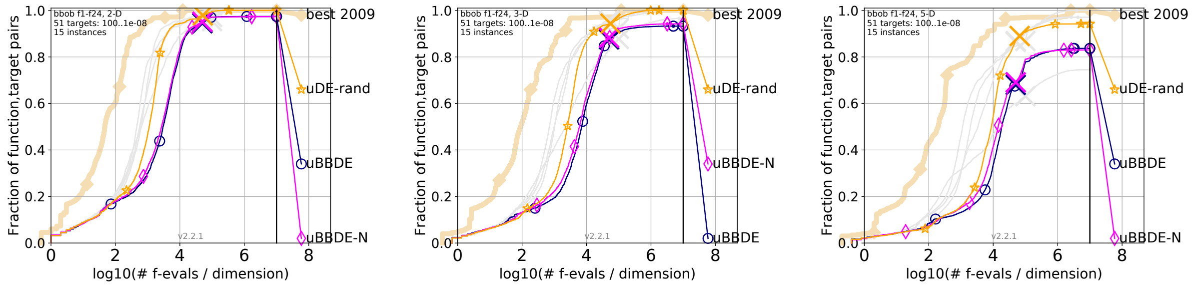

(a) Dimension 2 (b) Dimension 3 (c) Dimension 5

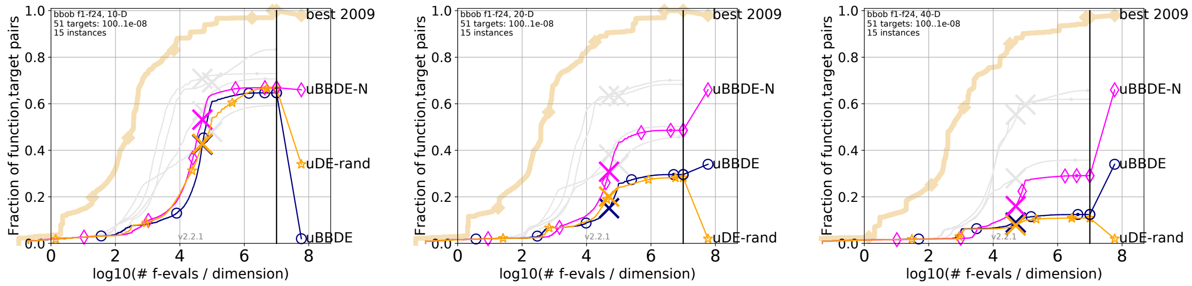

(d) Dimension 10 (e) Dimension 20 (f) Dimension 40

Figure 3: ECDFs of simulated (bootstrapped) runtimes of the 'rand' strategy for different problem dimensions (see [1] for more details), where the yellow line indicates the unbounded DE/rand, the purple line the unbounded BBDE-N, and the blue line the unbounded BBDE.

Separable ellipsoid, f_2, dimension 10 Separable ellipsoid, f_2, dimension 20

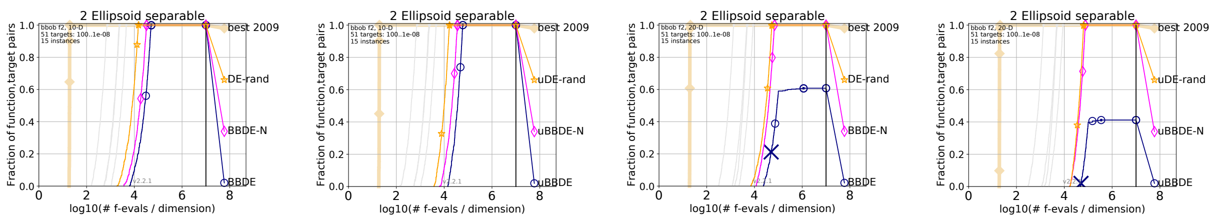

(a) Bounded decision space (b) Unbounded decision space (c) Bounded decision space (d) Unbounded decision space

Rotated ellipsoid, f_{10}, dimension 10 Rotated ellipsoid, f_{10}, dimension 20

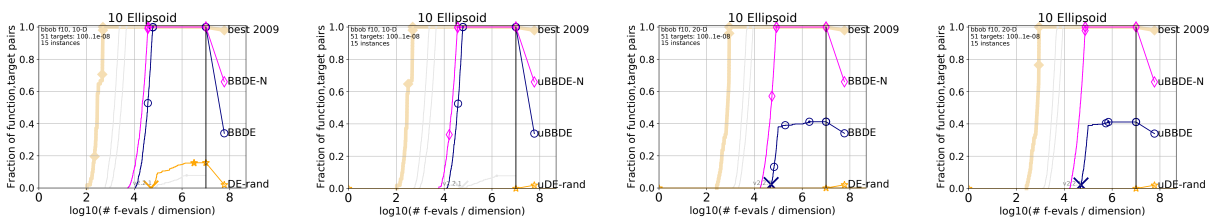

(e) Bounded decision space (f) Unbounded decision space (g) Bounded decision space (h) Unbounded decision space

Figure 4: ECDFs of simulated (bootstrapped) runtimes of the 'rand' strategy for the separable (top line) and rotated (bottom line) ellipsoid in dimensions 10 (first two columns) and 20 (last two columns). The yellow line indicates DE/rand, the purple line BBDE-N, and the blue line BBDE (see [1] for more details). Plots (a), (c), (e) and (g) show the performance of the algorithms on the bounded decision space, while the remaining plots (b), (d), (f) and (h) on the unbounded decision space.

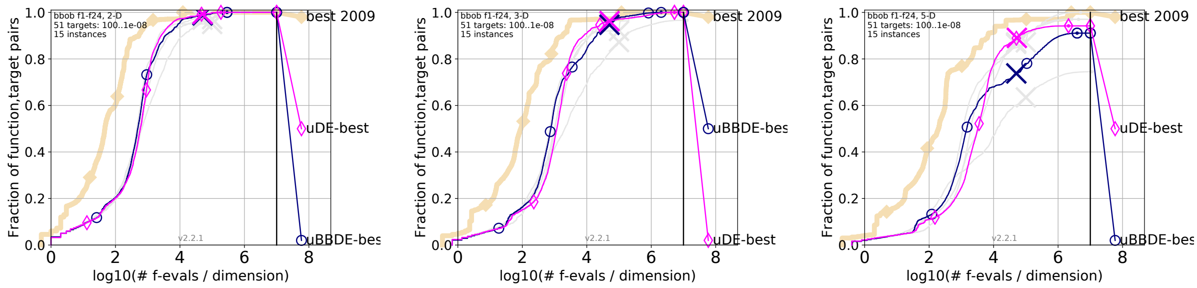

(a) Dimension 2 (b) Dimension 3 (c) Dimension 5

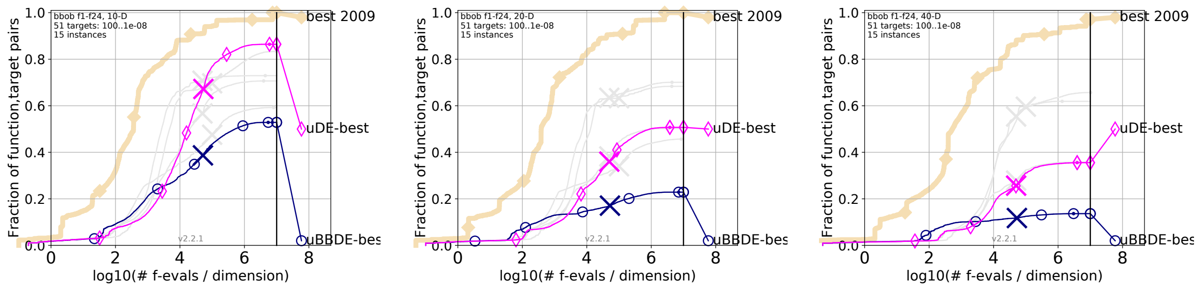

(d) Dimension 10 (e) Dimension 20 (f) Dimension 40

Figure 5: ECDFs of simulated (bootstrapped) runtimes of the ‘best’ strategy for different problem dimensions (see [1] for more details), where the purple line indicates the unbounded DE/best, and the blue line the unbounded BBDE/best.

Separable ellipsoid, f_2, dimension 10 Separable ellipsoid, f_2, dimension 20

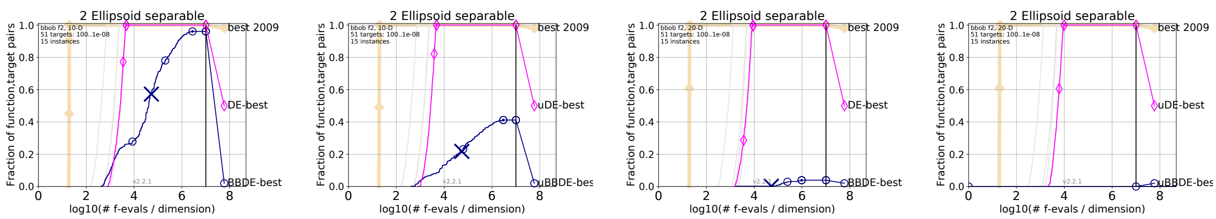

(a) Bounded decision space (b) Unbounded decision space (c) Bounded decision space (d) Unbounded decision space

Rotated ellipsoid, f_{10}, dimension 10 Rotated ellipsoid, f_{10}, dimension 20

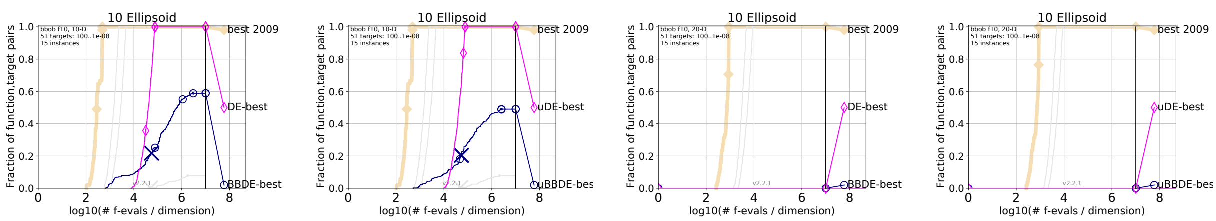

(e) Bounded decision space (f) Unbounded decision space (g) Bounded decision space (h) Unbounded decision space

Figure 6: ECDFs of simulated (bootstrapped) runtimes of the ‘best’ strategy for the separable (top line) and rotated (bottom line) ellipsoid in dimensions 10 (first two columns) and 20 (last two columns). The yellow line indicates DE/rand, the purple line BBDE-N, and the blue line BBDE (see [1] for more details). Plots (a), (c), (e) and (g) show the performance of the algorithms on the bounded decision space, while the remaining plots (b), (d), (f) and (h) on the unbounded decision space.

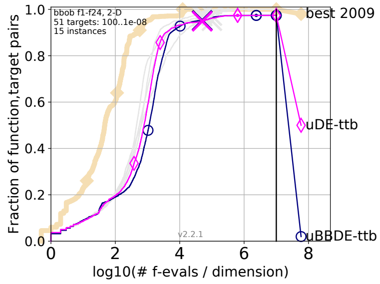

(a) Dimension 2

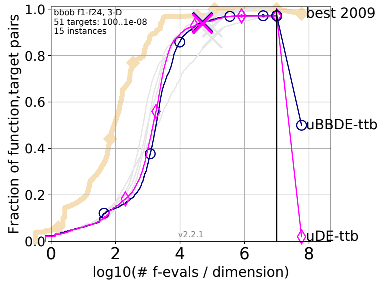

(b) Dimension 3

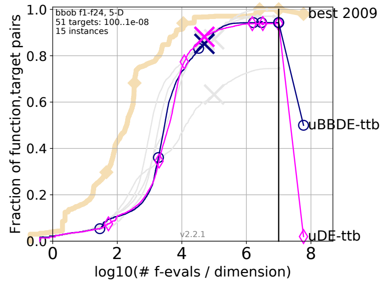

(c) Dimension 5

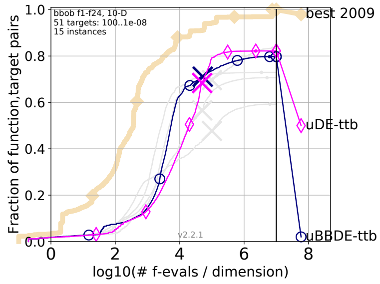

(d) Dimension 10

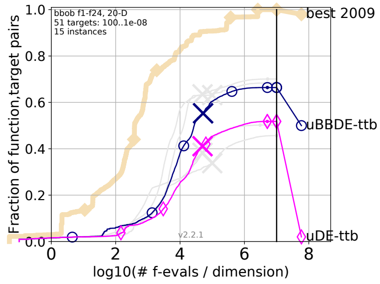

(e) Dimension 20

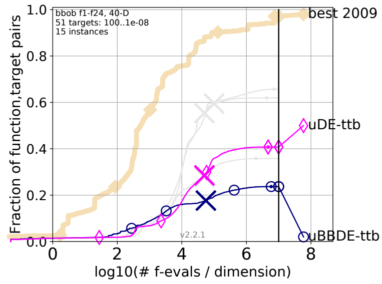

(f) Dimension 40

Figure 7: ECDFs of simulated (bootstrapped) runtimes of the 'target-to-best' strategy for different problem dimensions (see [1] for more details), where the purple line indicates the unbounded DE/target-to-best, and the blue line the unbounded BBDE/target-to-best.

Separable ellipsoid, f_2, dimension 10

Separable ellipsoid, f_2, dimension 20

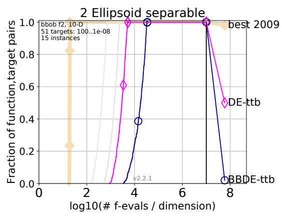

(a) Bounded decision space

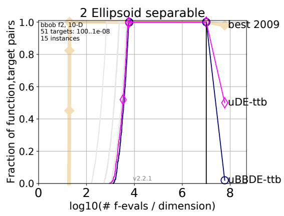

(b) Unbounded decision space

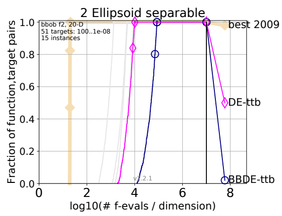

(c) Bounded decision space

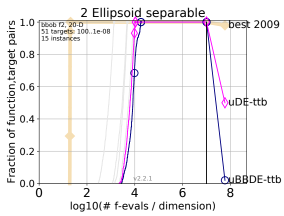

(d) Unbounded decision space

Rotated ellipsoid, f_{10}, dimension 10

Rotated ellipsoid, f_{10}, dimension 20

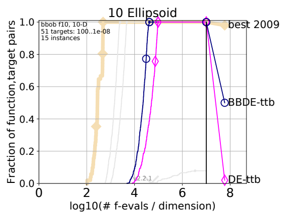

(e) Bounded decision space

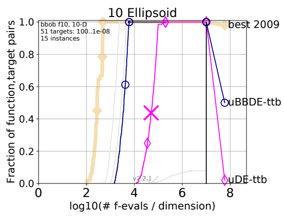

(f) Unbounded decision space

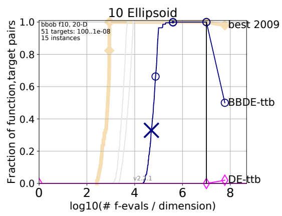

(g) Bounded decision space

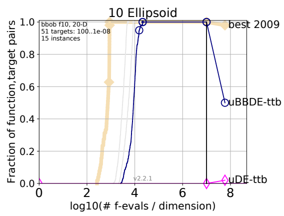

(h) Unbounded decision space

Figure 8: ECDFs of simulated (bootstrapped) runtimes of the 'target-to-best' strategy for the separable (top line) and rotated (bottom line) ellipsoid in dimensions 10 (first two columns) and 20 (last two columns). The yellow line indicates DE/rand, the purple line BBDE-N, and the blue line BBDE (see [1] for more details). Plots (a), (c), (e) and (g) show the performance of the algorithms on the bounded decision space, while the remaining plots (b), (d), (f) and (h) on the unbounded decision space.

indeed invariant to rotation on the ellipsoid problem. In addition, we corrected the pseudocode describing 'target-to-best' variants, since they were written incorrectly in the original work.

Acknowledgment

We acknowledge financial support from the Slovenian Research Agency (young researcher program, project no. Z2-8177, and research core funding no. P2-0209). This work is also part of a project that has received funding from the European Union's Horizon 2020 research and innovation program under grant agreement no. 692286.

References

[1] A. Vodopija, T. Tušar, and B. Filipič, "Comparing black-box differential evolution and classic differential evolution," in *GECCO '18 Companion: Genetic and Evolutionary Computation Conference Companion.* ACM, 2018, to appear.

[2] K. V. Price, "How symmetry constrains evolutionary optimizers," in *Proceedings of the IEEE Congress on Evolutionary Computation (CEC 2017).* IEEE, 2017, pp. 1712–1719.

[3] K. V. Price, R. M. Storn, and J. A. Lampinen, *Differential Evolution.* Springer, 2005, pp. 139–156.

[4] N. Hansen, A. Auger, O. Mersmann, T. Tušar, and D. Brockhoff, "COCO: A platform for comparing continuous optimizers in a black-box setting," *ArXiv e-prints*, vol. arXiv:1603.08785, 2016.

[5] S. Finck, N. Hansen, R. Ros, and A. Auger, "Real-parameter black-box optimization benchmarking 2010: Noiseless functions definitions," INRIA, Saclay, France, Tech. Rep. RR-6829, 2014.